Engineering Science and Technology, an International Journal 21 (2018) 760–768

HOSTED BY

Contents lists available at ScienceDirect

Engineering Science and Technology, an International Journal

journal homepage: www.elsevier.com/locate/jestch

Full Length Article

Application of Digital Image Correlation technique to Erichsen Cupping Test

Murat Aydin [a,*], Xin Wu [b], Kerim Cetinkaya [a], Mustafa Yasar [a], Ibrahim Kadi [a]

[a] Department of Industrial Design Engineering, Karabuk University, 78050 Karabuk, Turkey
[b] Department of Mechanical Engineering, Wayne State University, Detroit, MI, USA

ARTICLE INFO

Article history:
Received 30 January 2018
Revised 20 May 2018
Accepted 4 June 2018
Available online 20 June 2018

Keywords:
Digital Image Correlation
Erichsen Cupping Test
Stretch forming

ABSTRACT

Digital Image Correlation (DIC) technique is a powerful and useful tool in many industrial applications for both scientific and commercial purposes. It has been widely used for mechanical tests to understand the behaviour of material. In this study, 3D DIC technique was adopted to Erichsen Cupping Test (ECT) to measure the fracture cup height and demonstrate its benefits over traditional measurement techniques. Ck75 steel sheet with various material thickness was used in the experiments. The flat specimens were fixed in a closed die set-up and stretched along two directions until fracture. All the experiments were performed on a manually operated hydraulic press with a constant cross-head displacement and recorded with high resolution cameras. Finally, to determine the fractured cup heights, the accurate and satisfactory results were obtained through DIC measurements. The full-field thickness distribution and the maximum fracture forces were also determined.

1. Introduction

Digital Image Correlation (DIC), also known as white light speckle technique, is a non-contact optical measurement technique which is based on the comparison of deformed and un-deformed digital images in order to determine the whole filed displacement measurements on the surface of any object under various loading conditions [1–3].

Over the years, many studies have been carried out on image processing and the recent studies have been focused on the usage of Digital Image Correlation technique adopted material testing experiments for understanding the mechanical behaviour of materials. Peters and Ranson [4] proposed a technique that includes a comparison of deformed and un-deformed images for small fields and determined the position of those during loading conditions by capturing the reflected ultra-sonic waves. Sutton et al. [5] developed numerical algorithms and performed preliminary experiments using optically recorded images to show that 2D Digital Image Correlation is suitable when using optically recorded images. Pan et al. [6,7] combined the 2D DIC technique with high spatial resolution microscopes for both microscale and nanoscale deformation measurements and expressed that mean intensity gradient is an easy and effective global parameter to specify the quality of speckle pattern. Chen et al. [8] performed three-point bending tests with 3D DIC measurement technique to determine the mechanical properties of Bovine Bone and demonstrated that the deflection-force relationship was almost linear prior to reaching the peak strength. Bai et al. [9] developed an optical extensometer to estimate the local uniform strain on planar surface using large format lenses and image sensors. They performed uni-axial tensile experiments to validate the DIC results and found out that the resolution of the optical extensometer is achieved in between 2 and 3 $\mu\varepsilon$. Gencturk et al. [10] performed ultimate load tests on a full-scale pre-stressed I-shaped beam to calculate the full field 3-D displacement and compared DIC with traditional measurement results. They proved that the DIC technique gave a very accurate and detailed information and it was impossible to obtain through traditional techniques. Wang et al. [11] combined a generic stereo finite element model updating approach and stereo DIC to determine the plastic anisotropy of sheet materials by applying their approach to the Erichsen Cupping Test. They found out that the friction coefficient between the punch and the sheet could be identified. Li et al. [12] investigated the formability of tailor welded blanks by both numerically and experimentally. They used DIC and the Erichsen Cupping Test to investigate the influence of welding process on the strain distrubiton. They showed that experimental and numerical results gave good aggrement. Ashwini

* Corresponding author.
E-mail addresses: murataydin@karabuk.edu.tr (M. Aydin), xin.wu@wayne.edu (X. Wu), kcetinkaya@karabuk.edu.tr (K. Cetinkaya), myasar@karabuk.edu.tr (M. Yasar), ibrahimkadi@karabuk.edu.tr (I. Kadi).

Peer review under responsibility of Karabuk University.

https://doi.org/10.1016/j.jestch.2018.06.004
2215-0986/

et al. [13] studied on the integrated pattern matching method for quality testing of sheet materials by DIC. They pointed out that the reasonably stable and good results were achieved using the developed system and consistent acceptable outputs over various kinds of real life images had showed robustness of it. Poozesh et al. [14] installed a multi-camera 3D DIC measurement system in order to determine resonant frequencies and corresponding operating shapes of an individual wind turbine blade placed in a cantilevered boundary condition. They showed that multi-camera 3D DIC system has the capability to identify the whole dynamic behavior of wind turbine blades. Wang et al. [15] developed a multi-camera stereo DIC system to obtain whole displacement and strain fields of a metal specimen subjected to an Erichsen Cupping Test. They presented that the geometry and the displacement fields of the deformed specimens were stitched and strain fields of the surface were obtained.

Traditional measurement instruments provide only average value in material testing and these average values are not enough to understand the mechanical behaviour of materials. However, DIC can calculate the full field strain and displacement distributions and mechanical properties of both metal and non-metal materials. Zhou et al. [16] determined the mechanical properties of flexible packaging material in tensile test using DIC technique. They showed the advantages of DIC such as non-contact, no reinforced effect, high precision over entire field, wide measurement range, and good measurement stability. Grytten et al. [17] also used 3D DIC to calculate the strain and displacement fields of rectangular cross-section of a talc and elastomer modified polypropylene compounds in uni-axial tensile test. They showed that the isochoric assumption is invalid and the transverse contraction had to be measured to obtain the true stress using 3D DIC. Qoubaa [18] and Othman studied the mechanical behaviour of Polyetheretherketone in tensile test at room temperature under various strain rates in order to determine the impact strain rate range using DIC. Heinz [19] calculated the yield strain, Poisson's ratio and compression modulus of glassy polymer using 3D DIC technique. He suggested that DIC is a practical technique to understand non-uniform strain distribution before yielding. Dudescu et al. [20] used DIC technique to determine the pre and post yield regime and rate dependent on the deformation properties of polyvinylchloride (PVC) in uniaxial tensile test under various crosshead speeds. They revealed that strain rate has an insignificant influence on true strain–stress curves for small strain rates as compared to higher strain rates. Hwang et al. [21] used a modified coarse fine iterative DIC technique to measure the strain and displacement fields for several reinforced aluminium specimens. They recognized that the developed technique could cover the whole strain fields of those specimens even under high elongation.

In the light of above literature review, the current study has been carried out to demonstrate the capability and benefits of DIC technique in two-dimensional stretching experiments (ECT) rather than in uni-axial tensile test. The ECT was performed using flat specimen with various sheet thicknesses. Thus, determining the Erichsen Index number dependenting on the sheet material thickness and obtaining the full-field material thickness distribution were aimed by applying DIC technique. In order to validate DIC results, the physical measurement instrument were used.

2. Materials and method

2.1. Materials

In this study, Ck75 steel, also known as SAE 1074 in USA standard [22], was used in Erichsen Cupping Test. Three different material thicknesses, 0.40 mm, 0.50 mm, and 0.60 mm were chosen in order to determine the Erichsen Index number. The mechanical properties as well as the chemical composition were obtained from the manufacturer. In Fig. 1, the tensile curves of test material in each rolling directions are given. Tables 1 and 2 show the chemical composition and average mechanical properties of test materials for three rolling directions [23].

As it can be seen from Table 2, ρ defines the density, E defines the Young's modulus, $R_{p0.2}$ defines the yield strength, R_m defines the ultimate tensile strength, n defines the strain hardening exponent.

2.2. Method

In the forming experiments, the ball punch deformation test, well known as Erichsen Cupping Test was used to stretch the flat specimens until fracture in order to determine the ductile behaviour of metallic sheet materials. The forming test consisted of biaxial stretching of a fully constrained test specimen that was circular or square flat piece. All tooling and experiment specimens were designed according to ASTM E643-15 standard [24]. In order to fully constraint the flat specimens, the die set was designed as two parts, one was outer ring that had inner screw (M90 × 2 mm) and the latter, middle part had the outside screw (M90 × 2 mm). By means of rotating the middle part, flat specimens were fixed on the die surface with the help of friction. Fig. 2 shows the schematic view of Erichsen tooling set-up. The Table 3 describes the dimensions of the test tools. During the experiments, commercial grease was used as a lubricant and it was applied on the top of punch in each test.

The forming experiments were performed on the manually operated hydraulic press which has 380 mm stroke and flow control valve that regulates the velocity of punch. The cross-head displacement was set to a rate of 0.1 mm/s with flow control valve. All the forces were measured with Zemic HM2D4 5t load cell. Output sensitivity of load cell was 2.0 ± 0.002 mV/V. Output voltages of the load cell were converted into kilograms by weight indicator and forces were saved using modbus protocol of weight indicator. The sampling rate of modbus protocol was set as 1000 samples per second. Fig. 3 shows the hydraulic press with mounted load cell and closed die set-up.

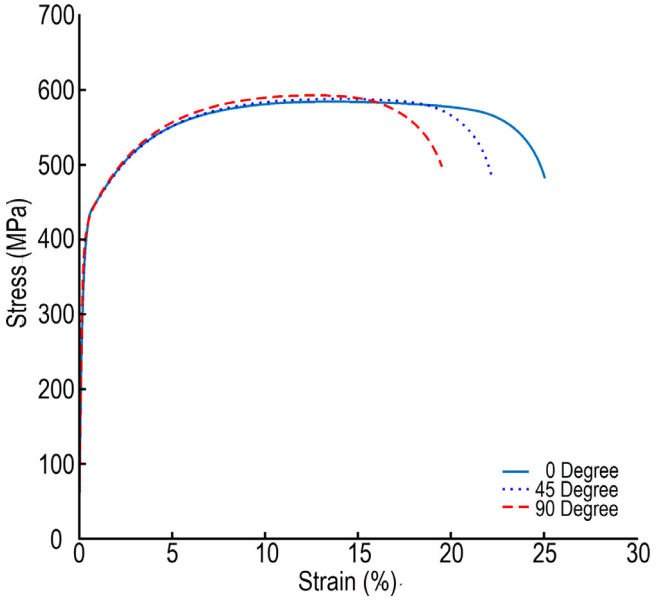

Fig. 1. Tensile test curves for Ck75 in various rolling directions.

Table 1
Chemical properties of Ck75 [23].

C (%)	Si (%)	Mn (%)	P (%)	S (%)	Al (%)	Cr (%)	Mo (%)	Cu (%)	Ni (%)
0.761	0.241	0.608	0.009	0.001	0.033	0.161	0.004	0.034	0.042

Table 2
Mechanical properties of Ck75 [23].

Sample Direction	ρ (kg/m^3)	E (GPa)	$R_{p0.2}$ (MPa)	R_m (MPa)	n (–)
0° Longitudinal	7.85	205	399	576	0.149
45° Diagonal	7.85	205	413	590	0.150
90° Transversal	7.85	205	409	593	0.156

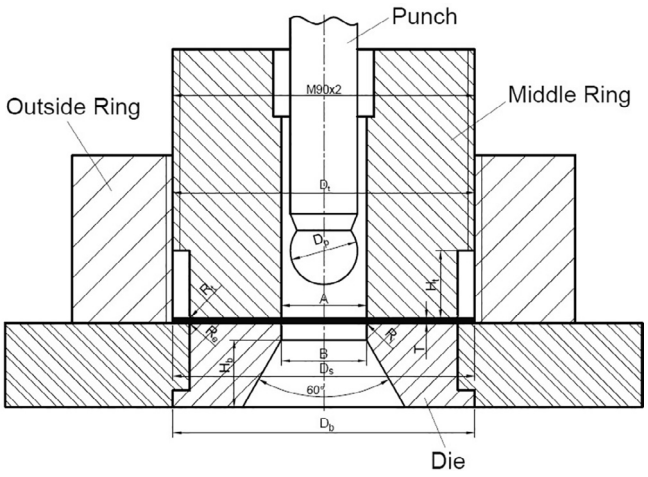

Fig. 2. Schematic view of Erichsen set-up [24].

Table 3
Dimensions of Erichsen Cupping Test set-up [24].

Symbol	Definition	Dimensions mm
T	Thickness of test specimen	Full thickness
D_p	Diameter of spherical end of penetrator	20 ± 0.05
A	Bore diameter of bottom die	25.4 ± 0.1
B	Bore diameter of top die	25.4 ± 0.1
D_t	External diameter of top die	90 ± 0.1
D_b	External diameter of top die	90 ± 0.1
D_s	Width of test specimen	89
R_i	Corner radius of interior bottom die	0.81 ± 0.05
R_e	Corner radius of exterior bottom die	0.81 ± 0.05
R_t	Corner radius of exterior top die	0.81 ± 0.05
H_b	Thickness of bottom die	20
H_t	Thickness of top die	20

Nowadays, due to enhancements in optical technology, many of the digital cameras have been started using CMOS sensors and those have been widely used in DIC measurement [25–28]. Two Nikon D90 digital cameras with 18–105 mm lenses and a resolution of 1280 × 720 pixels with 24 frames per second, focal length of 50 mm, and an aperture of f/1.8 were used to monitor and record the whole process during the experiments. Fig. 4a shows the camera setup that was located under the press plate.

DIC technique needs the special painting process based on creating random speckle pattern which are black dots against white background. By using this technique, it is possible to create a non-uniform and random surface texture in order to track the full-field displacement measurement [29]. In ECT test, specimens were prepared with 149 mm × 120 mm dimensions in order to

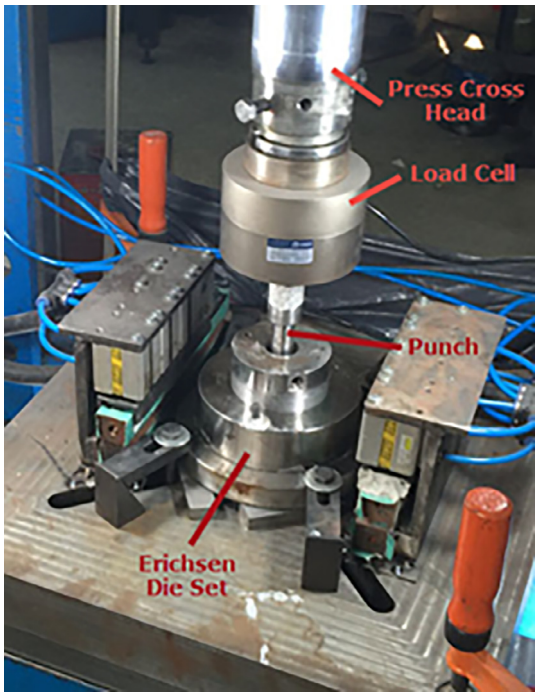

Fig. 3. Hydraulic press and closed die set-up.

place them in a closed die set quickly and easily. Before each test, all the specimens were sanded with 320 grinding paper to remove any dirt and corrosion. After grinding process, all the specimens were cleaned with the acetone. When the cleaning process was completed, the specimens were painted with matt cellulosic white paint as a background to improve the adhesion on the metal surface and to prevent any reflection errors. After applying white paint, matt black speckles were splashed on the specimen's surface to obtain the random speckle pattern. Fig. 4b shows an example of painted ECT specimen. All the experiments were carried out at room temperature and laboratory environment. In order to improve the measurement accuracy, prevent the shadow errors on the specimen's surface, and to achieve the clear focus during testing, the cold white lights were directed onto the specimen.3D DIC technique needs a calibration process to calculate the displacement and strain, whereas 2D DIC systems do not [17,29]. During the experiments, calibration processes were performed at the beginning of tests to achieve the accurate and precise results. 12 × 9 circular dots with 8 mm spacing were printed by using high resolution laser printer and bonded on a flat alumina plate. This plate was translated and moved in the measurement field that

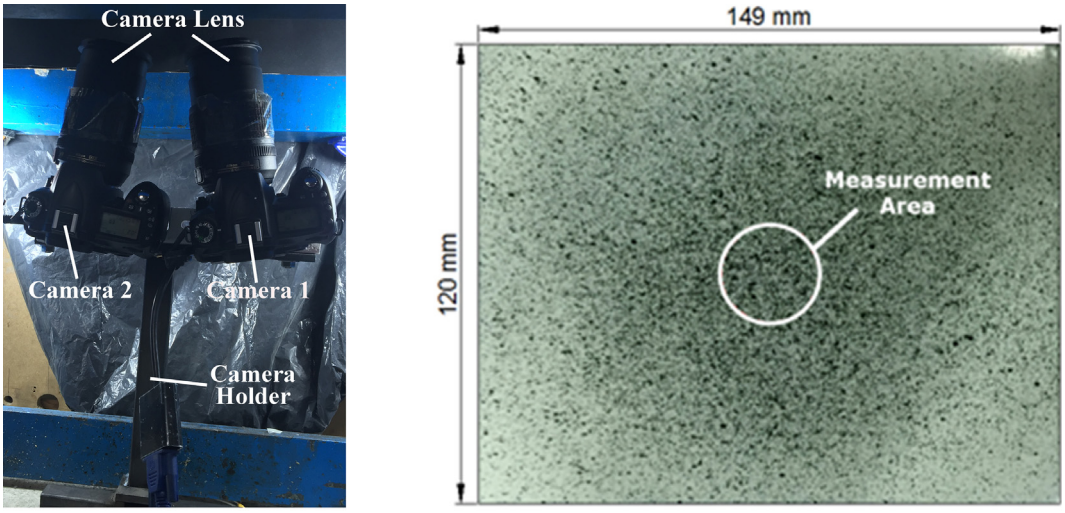

Fig. 4. DIC setup. (a) Camera orientation, (b) Example of painted specimen.

was in the same position of specimen and both cameras captured several images for calibration. Fig. 5 shows the calibration plate.

Currently, there are many Digital Image Correlation softwares and codes in the market and one of those is Vic3D. It is easy to use software to process images and calculate the displacement and strain fields of flat specimens as 3D. All the images in the experiments were processed using Vic3D software.

3. Results and discussion

The maximum height of material before the initial crack was measured by using Vic3D DIC software and the maximum load was measured using load cell. In order to validate the DIC results, the height of the fractured specimens were measured using digital height gauge with 0.01 mm sensitivity. The example of height gauge measurement for the each thicknesses is shown in Fig. 6. In Table 4, the DIC and height gauge measurements are given according to the sheet thickness and the DIC average cup height values.

It can be seen from Table 4 that the height of the fractured specimens were measured 4.41 mm for 0.4 mm sheet thickness, 4.78 mm for 0.5 mm sheet thickness, and 5.04 mm for 0.6 mm sheet thickness. Besides, the Erichsen Index (EI) number measured with DIC is varying between 4.353 mm and 4.356 mm for 0.4 mm sheet thickness, 4.724 mm and 4.727 mm for 0.5 mm sheet thickness,

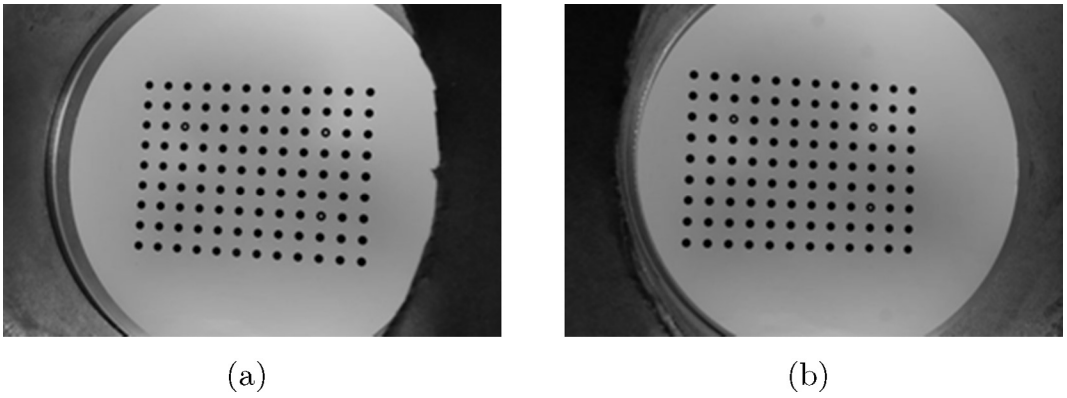

Fig. 5. Calibration plate. (a) Camera 1, (b) Camera 2.

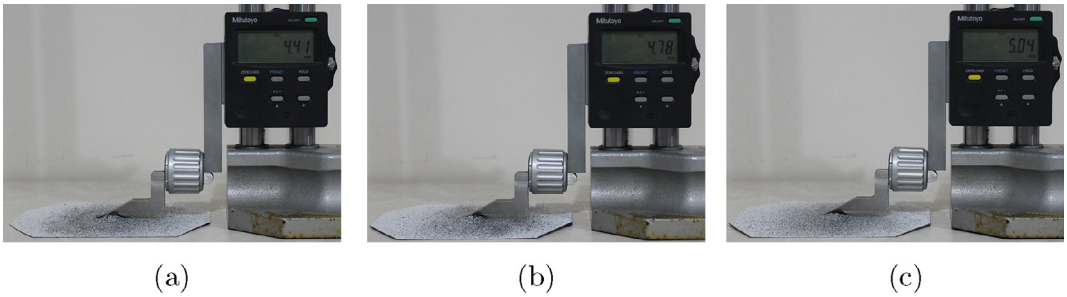

Fig. 6. Height gauge measurement, (a) 0.40 mm for Specimen No.1, (b) 0.50 mm for Specimen No.2, (c) 0.60 mm for pecimen No.3.

Table 4
Fractured cup heights measured by height gauge and DIC.

Thickness (mm)	Specimen	Height Gauge (mm)	DIC Cup Height (mm)	DIC Average Height (mm)
0.40	No.1	4.41	4.35668	4.35491
	No.2	4.41	4.35303	
	No.3	4.41	4.35503	
0.50	No.1	4.78	4.72719	4.72607
	No.2	4.78	4.72406	
	No.3	4.78	4.72697	
0.60	No.1	5.04	4.98543	4.98618
	No.2	5.04	4.98808	
	No.3	5.04	4.98503	

and 4.985 and 4.988 for 0.6 mm sheet thickness. In addition, the average cup heights were calculated as 4.35491 mm, 4.72607 mm, and 4.98618 mm for 0.4 mm, 0.5 mm, and 0.6 mm sheet thicknesses, respectively. The findings indicate that the fractured cup height measurements for both DIC and height gauge, Erichsen Index number, increases with increasing the sheet thickness. In addition, according to the comparison of the DIC and the digital height gauge measurements, it is seen that the digital height gauge measurements are slightly higher than the DIC and the difference between two measurement methods is varying from 0.05192 mm to 0.05697 mm for each experiments.

From DIC results, the fractured cup height measurements for specimen having various sheet thicknesses are given in Figs. 7–9, respectively. As it can be seen from the figures, each set of images

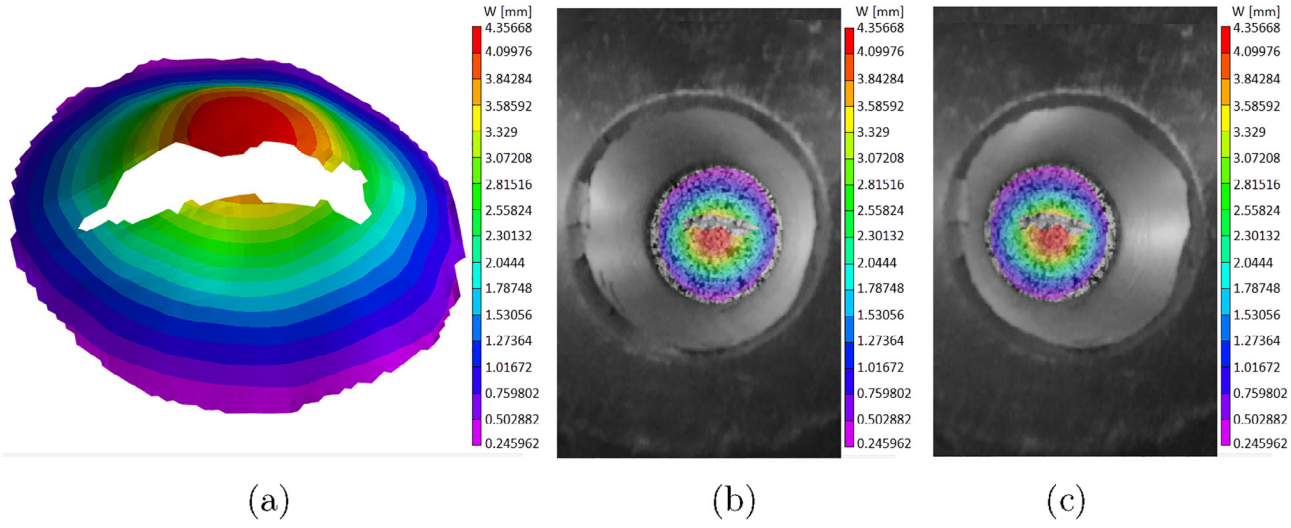

Fig. 7. DIC fractured cup height measurement of 0.40 mm sheet thickness for Specimen No.1. (a) 3D Plot, (b) Camera 1, (c) Camera 2.

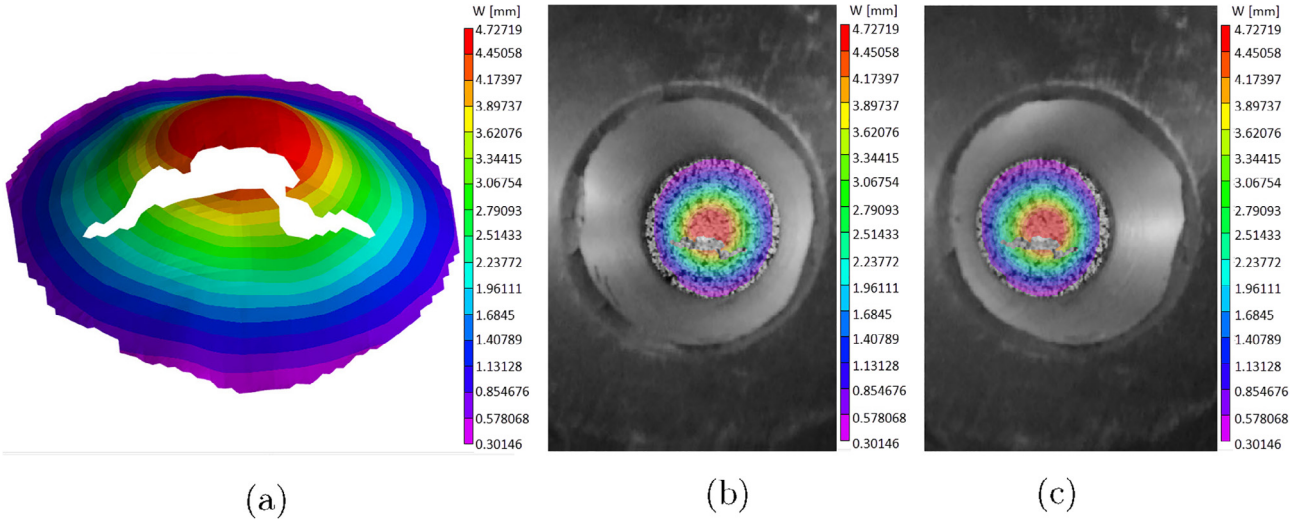

Fig. 8. DIC fractured cup height measurement of 0.50 mm sheet thickness for Specimen No.1 (a) 3D Plot, (b) Camera 1, (c) Camera 2.

includes the 3D plot data which shows 3D dome height shape of the sheet at the exact fracture moment, the camera 1 and the camera 2 views. The color scale bar given on the right side of the images is indicating the fractured cup height value (W) in millimeter.

The maximum fractured cup height is measured as 4.35668 mm for 0.40 mm sheet thickness and demonstrated as a dome height in Fig. 7(a). As it can be seen from the figure that maximum dome height is shown as red zone which is at the top of the punch and

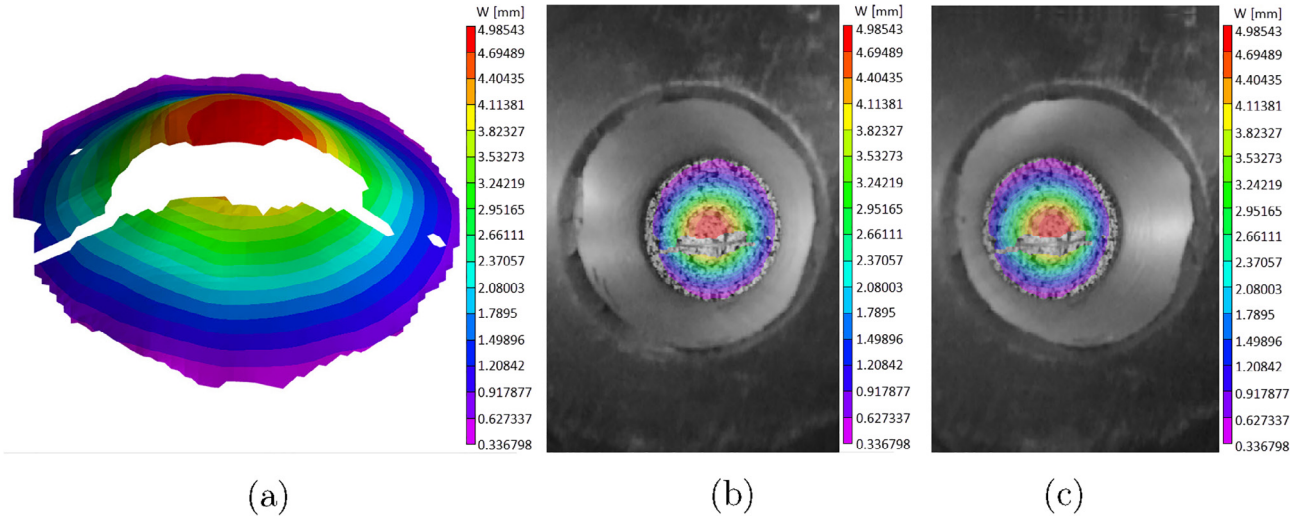

Fig. 9. DIC fractured cup height measurement of 0.60 mm sheet thickness for Specimen No.1 (a) 3D Plot, (b) Camera 1, (c) Camera 2.

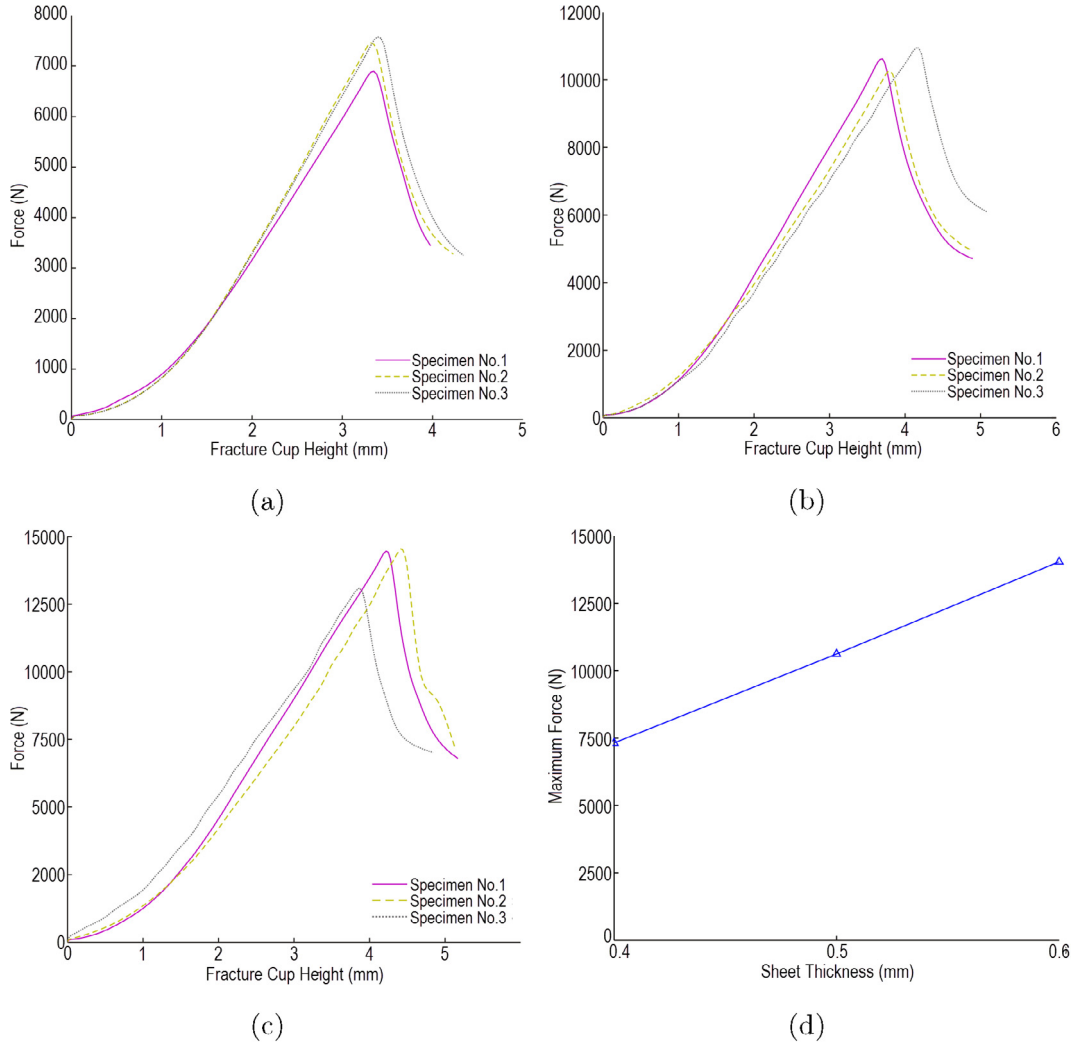

Fig. 10. Force measurements for (a) 0.40 mm, (b) 0.50 mm, (c) 0.60 mm, and (d) Average maximum force vs. sheet thickness.

the minimum displacement of the sheet achieved at the bore diameter as 0.245962 mm and this field is presented as purple. Because of the fracture on the sheet, the contrast of the subset disappeared and the bad correlation was removed on the cracked edge. So, this field was demonstrated as non-color in 3D plot and also in grey color from the view of the Camera 1 and Camera 2.

When the sheet thickness is increased to 0.50 mm, the maximum dome height is measured as 4.72719 mm and minimum displacement of the sheet as 0.30146 mm (see in Fig. 8). For 0.60 mm sheet thickness, the fractured cup height is about 4.98543 mm which is the maximum value of all experiments and minimum displacement of the sheet is about 0.336798 mm where the position was close to the bore diameter of the die edge (see in Fig. 9). From these results, it can be seen that the fractured cup height and forming limits are increased by an increment in the sheet thickness from 0.4 mm to 0.6 mm.

The measured force values are given in Fig. 10(a–c) as a function of fractured cup heights for each specimens (No.1, No.2, No.3) for all sheet thicknesses (0.40 mm, 0.50 mm, 0.60 mm, respectively). In Fig. 10(a), the maximum forces are measured as 6914.9 N, 7466.2 N, and 7578.3 N for specimen No.1, No.2 and No.3, respectively. When the sheet thickness was increased to 0.50 mm, the maximum forces are measured as 10633.0 N, 10272.0 N, and 10966.0 N. While the sheet thickness was increased to 0.60 mm, the maximum forces are determined as 14459.0 N, 14566.0 N, and 13100.0 N. From these results, the average maximum forces are about 7319.8 N for 0.40 mm, 10623.67 N for 0.5 mm, and 14041.67 N for 0.6 mm. It can be seen that the maximum forces

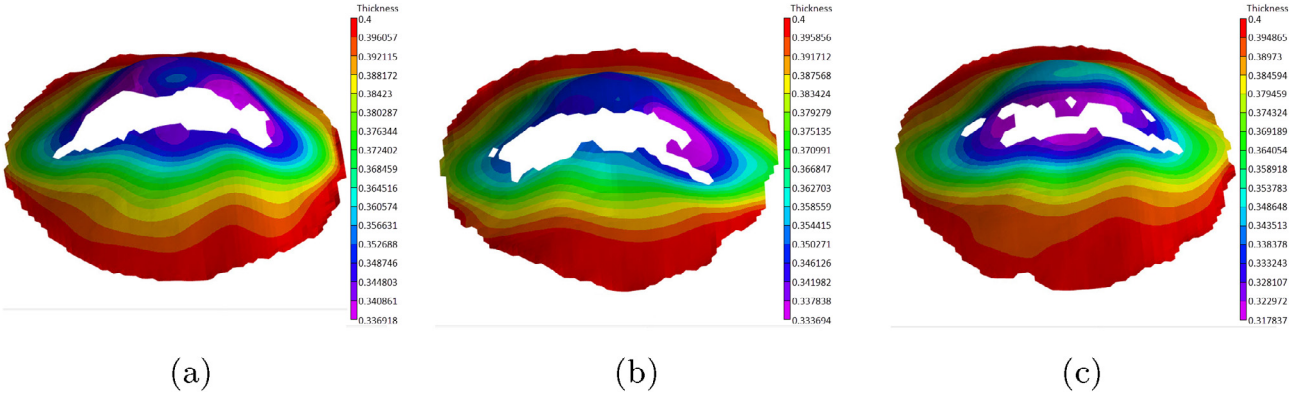

Fig. 11. DIC sheet thickness distribution measurement of 0.40 mm specimens (a) Specimen No.1, (b) Specimen No.2, (c) Specimen No.3.

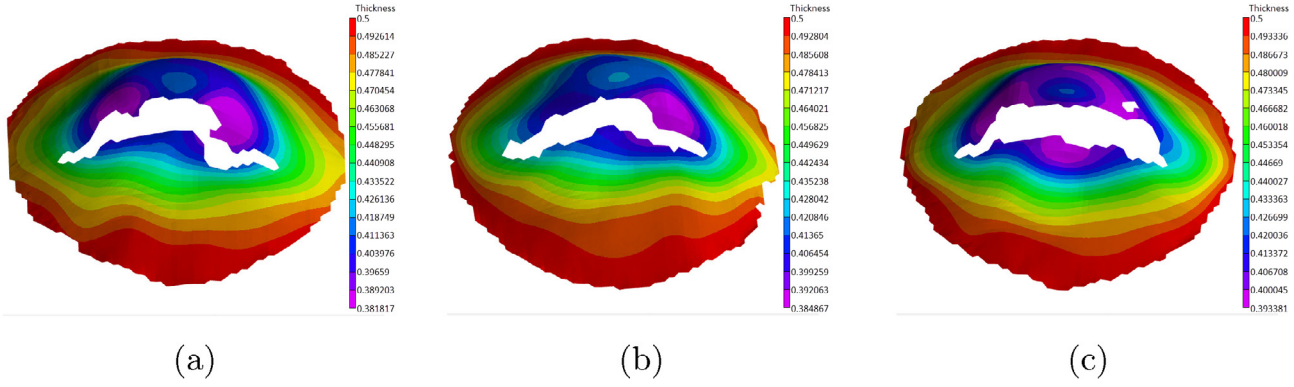

Fig. 12. DIC sheet thickness distribution measurement of 0.50 mm specimens (a) Specimen No.1, (b) Specimen No.2, (c) Specimen No.3.

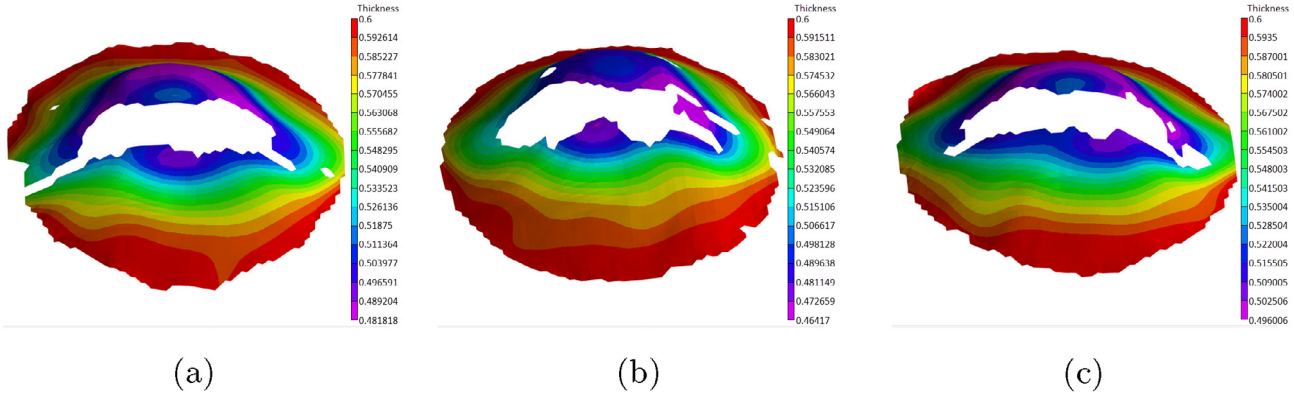

Fig. 13. DIC sheet thickness distribution measurement of 0.60 mm specimens (a) Specimen No.1, (b) Specimen No.2, (c) Specimen No.3.

and fracture cup heights increase in relation to sheet thickness as seen in Fig. 10(d).

DIC technique can calculate not only the cup height measurements but also the sheet thickness distribution of the sheet material. The sheet thickness distributions after fracture are given in Figs. 11–13 for all sheet thicknesses of each specimen.

As it can be seen from figures (Figs. 11–13), the fractures occured at the top of the punch are indicated in purple color where the maximum thinning is located. In Fig. 11, the minimum thickness is calculated as 0.336918 mm, 0.333694 mm, and 0.317837 mm for Specimen No.1, No.2, and No.3 of 0.4 mm sheet thickness respectively. In addition, for 0.5 mm sheet thickness, the minimum thickness is obtained as 0.381817 mm, 0.384867 mm, and 0.393381 mm for Specimen No.1, No.2, and No.3, respectively (see in Fig. 12). Moreover, when the sheet thickness was increased to 0.6 mm, the minimum thickness achieved as 0.481818 mm, 0.46417 mm, and 0.496006 mm for the same specimens (see in Fig. 13). It can be seen that the minimum thickness after fracture increased depending on the increasing sheet thickness. For all experiments, minimum thinning was occured on the cracked line of the fractured specimens.

4. Conclusion

This study presents the adoption of DIC technique to the traditional Erichsen Cupping Test in order to measure the cup height and determine the exact fracture height of the specimens (Erichsen Index number) experimentally and proves to be an easy and a flexible technique. Flat steel specimens with various thicknesses were constrained in a closed die set and deformed with a constant crosshead speed until the fracture occured while two high definition cameras were recording the whole process. The deformed and undeformed images were processed using Vic3D software. As a result;

1. DIC measurements gave the acceptable and satisfying results when it was compared with the height gauge measurement. The physical instrument measurements were slightly above the DIC measurements. Because, in the forming experiments, cross head of the manual operated hydraulic press was still moving a little further although it was stopped immediately when the crack was observed from external monitors. In addition, in the DIC measurement, for a second, 24 frames were obtained and the frame which was the beginning of the fracture were used. Besides, the commercial CMOS cameras are useful in laboratory environment[25].
2. Measured cup heights increased with increasing the sheet thickness (see Table 4). When the specimen thickness was increased from 0.40 mm to 0.50 mm, the average fracture cup height increased dramatically to about 0.37116 mm. However, the average cup height of the sheet with 0.60 mm sheet thickness was increased by 0.26011 mm as compared to the sheet with thickness of 0.50 mm.
3. In terms of force measurement, the maximum forces and average maximum forces for each experiment were increased with (see Fig. 10) increasing the sheet thickness and cup heights. The average maximum force is calculated as 7319.8 N for 0.40 mm sheet thickness, 10623.67 N for 0.50 mm sheet thickness, and 14041.67 N for 0.60 mm sheet thickness.
4. From the experiments, the average minimum thickness is calculated as 0.329483 mm, 0.386688 mm, and 0.480665 mm for 0.4 mm, 0.5 mm, and 0.6 mm sheet thicknesses, respectively. It was also observed that the average minimum thickness also increased with increasing sheet thickness of the material.
5. Installed DIC setup can be applied to the Erichsen Cupping Test, precise measurement can be performed simultaneously through the forming operations. Besides, the same setup can be used in various deformation measurements in terms of non-contact, easy, flexible measurement requirement.

References

[1] T. Chu, W. Ranson, M.A. Sutton, Applications of digital-image-correlation techniques to experimental mechanics, Exp. Mech. 25 (3) (1985) 232–244, https://doi.org/10.1007/BF02325092.
[2] H. Bruck, S. McNeill, M. Sutton, W. Peters, Digital image correlation using newton-raphson method of partial differential correction, Exp. Mech. 29 (3) (1989) 261–267, https://doi.org/10.1007/BF02321405.
[3] D. Lecompte, A. Smits, S. Bossuyt, H. Sol, J. Vantomme, D. Van Hemelrijck, A. Habraken, Quality assessment of speckle patterns for digital image correlation, Opt. Lasers Eng. 44 (11) (2006) 1132–1145, https://doi.org/10.1016/j.optlaseng.2005.10.004.
[4] W. Peters, W. Ranson, Digital imaging techniques in experimental stress analysis, Opt. Eng. 21 (3) (1982), https://doi.org/10.1117/12.7972925. 213427–213427.
[5] M. Sutton, W. Wolters, W. Peters, W. Ranson, S. McNeill, Determination of displacements using an improved digital correlation method, Image Vision Comput. 1 (3) (1983) 133–139, https://doi.org/10.1016/0262-8856(83)90064-1.
[6] B. Pan, K. Qian, H. Xie, A. Asundi, Two-dimensional digital image correlation for in-plane displacement and strain measurement: a review, Meas. Sci. Technol. 20 (6) (2009) 062001, https://doi.org/10.1088/0957-0233/20/6/062001.
[7] B. Pan, Recent progress in digital image correlation, Exp. Mech. 51 (7) (2011) 1223–1235, https://doi.org/10.1007/s11340-010-9418-3.
[8] Y. Chen, D. Yang, Y. Ma, X. Tan, Z. Shi, T. Li, H. Si, Experimental investigation on the mechanical behavior of bovine bone using digital image correlation technique, Appl. Bionics Biomech. 2015 (1) (2015) 1–6, https://doi.org/10.1155/2015/609132.
[9] P. Bai, F. Zhu, X. He, Optical extensometer and elimination of the effect of out-of-plane motions, Opt. Lasers Eng. 65 (2015) 28–37, https://doi.org/10.1016/j.optlaseng.2014.04.010.
[10] B. Gencturk, K. Hossain, A. Kapadia, E. Labib, Y.-L. Mo, Use of digital image correlation technique in full-scale testing of prestressed concrete structures, Measurement 47 (2014) 505–515, https://doi.org/10.1016/j.measurement.2013.09.018.
[11] P.L.D.D. Yueqi Wang, Sam Coppieters, Anisotropic yield surface identification of sheet metal through stereo finite element model updating, Strain Anal. 51 (8) (2016) 598–611, https://doi.org/10.1177/0309324716666437.
[12] R.G. Yanhua Li, Jianping Lin, Numerical and experimental analysis on the formability of tailor welded blanks based on digital image correlation, in: AIP Conference Proceedings. doi:10.1063/1.4850084.
[13] P.P.K.P. Pagar Ashwini, Ahirrao Pooja, Integrated pattern matching algorithm for quality testing of sheet-metal using digital image processing, in: A Conference on Wireless Communication and Android Apps, WiCAA 15.
[14] N.C.A.P. Poozesh, J. Baqersad, A multi-camera stereo dic system for extracting operating mode shapes of large scale structures, Adv. Opt. Methods Exp. Mech. 3 (2016) 225–238, https://doi.org/10.1007/978-3-319-22446-629.
[15] L.P.C.S.H.P.D.D. Wang, Application of a multi-camera stereo dic set-up to assess strain fields in an erichsen test: Methodology and validation, Strain Int. J. Exp. Mech. 49 (2) (2013) 190–198, https://doi.org/10.1111/str.12027.
[16] J.-W. Zhou, D.-H. Liu, L.-Y. Shao, Z.-L. Wang, Application of digital image correlation to measurement of packaging material mechanical properties, Math. Problems Eng. 2013 (2013) 1–8, https://doi.org/10.1155/2013/204875.
[17] F. Grytten, H. Daiyan, M. Polanco-Loria, S. Dumoulin, Use of digital image correlation to measure large-strain tensile properties of ductile thermoplastics, Polym. Testing 28 (6) (2009) 653–660, https://doi.org/10.1016/j.polymertesting.2009.05.009.
[18] Z. El-Qoubaa, R. Othman, Tensile behavior of polyetheretherketone over a wide range of strain rates, Int. J. Polym. Sci. 2015 (2015) 1–9, https://doi.org/10.1155/2015/275937.
[19] S.R. Heinz, J.S. Wiggins, Uniaxial compression analysis of glassy polymer networks using digital image correlation, Polym. Testing 29 (8) (2010) 925–932, https://doi.org/10.1016/j.polymertesting.2010.08.001.
[20] C. Dudescu, A. Botean, M. Hardau, N. Bal, Measurement of thermoplastics tensile proprieties using digital image correlation, in: Proceedings of the 14th Symposium on Experimental Stress Analysis and Materials Testing.
[21] S.-F. Hwang, M.-C. Shen, B.-B. Hsu, Strain measurement of polymer materials by digital image correlation combined with finite-element analysis, J. Mech. Sci. Technol. 29 (10) (2015) 4189–4195, https://doi.org/10.1007/s12206-015-0913-4.
[22] S.S. Resources, International equivalents, 2017.http://steelstrip.co.uk/international-equivalents/.
[23] Waelzholz, The chemical and mechanical properties of ck75 steel strip, 2017.
[24] A. E643-15, Standard Test Method for Ball Punch Deformation of Metallic Sheet Material, 2015.

[25] X. Guo, J. Liang, Z. Xiao, B. Cao, Digital image correlation for large deformation applied in ti alloy compression and tension test, Optik-Int. J. Light Electron. Opt. 125 (18) (2014) 5316–5322, https://doi.org/10.1016/j.ijleo.2014.06.067.
[26] B. Pan, D. Wu, Y. Xia, An active imaging digital image correlation method for deformation measurement insensitive to ambient light, Opt. Laser Technol. 44 (1) (2012) 204–209, https://doi.org/10.1016/j.optlastec.2011.06.019.
[27] W. Wang, J.E. Mottershead, T. Siebert, A. Pipino, Frequency response functions of shape features from full-field vibration measurements using digital image correlation, Mech. Syst. Signal Process. 28 (2012) 333–347, https://doi.org/10.1016/j.ymssp.2011.11.023.
[28] B. Pan, D. Wu, Y. Xia, High-temperature deformation field measurement by combining transient aerodynamic heating simulation system and reliability-guided digital image correlation, Opt. Lasers Eng. 48 (9) (2010) 841–848, https://doi.org/10.1016/j.optlaseng.2010.04.007.
[29] Image Correlation for Shape, Motion and Deformation Measurements, Springer, 2009.